Microscopic Study of Nanostructured AlO_x

UV Laser Patterning Via Self-organized Nanospheres

Large area ordered nanopatterning of RF sputtered AlO_x layers have been carried out. The technique involves UV laser treating of the film through LB films of silica nanospheres. The hexagonal, close packed arrangement of these spheres was projected to the surface due to the laser treatment resulting in ordered structure of pits of ~200 nm diameter and 1.3 nm depths. The samples were characterized by means of AFM and XTEM. Experimental results are in good agreement with the simulations.

Introduction

Recently the nano-scale modification of materials received a wide interest in research. This includes nanopatterning that is applicable in many fields [1, 2, 3]. One of the most promising fields of nanopatterning is the development of bit patterned magnetic media (BPM). The main top-down techniques for the fabrication of ordered nanostructures are e-beam litography [4] and nanoimprinting [5]. The bottom-up techniques are mainly based on nanosphere lithography [6] and molecular self-assembly [7]. However, most of these methods suffer from the disadvantage of low throughput and high costs.

In this paper a fast and low-cost method is proposed to obtain ordered nanopatterns directly, or via preparation of masks and imprint molds for nanolithography. We apply a monolayer of self-assembled silica nanospheres, prepared by the Langmuir-Blodgett (LB) technique [8] that is a template for a single pulse UV-laser treatment of the sample. This technique can be applied under atmospheric conditions. The treatment of relatively large areas requires short time.

In this work amorphous aluminium-oxide layers have been nanostructured. AlO_x is a hard, durable non-reactive, high-melting point material that can be applied as (negative or positive) mask for nanolithography and as a mold for nanoimprinting [5].

Experimental

Amorphous AlO_x layers of 25 nm thickness were RF sputter deposited from an Al_2O_3 target onto single crystal Si substrates, at room temperature and at a rate of 0.25 Å/s. The sputtering gas was an $Ar–O_2$ mixture with the partial pressures of 1.6×10^{-2} mbar and 4×10^{-3} mbar, respectively. Subsequently, the films were covered with a monolayer of silica nanospheres of 300 nm diameter arranged in a hexagonal structure by the LB technique.

The silica nanoparticles and their LB films were prepared as reported elsewhere [9]. LB-films of the nanoparticles were prepared in a KSV 2000 film balance by vertical deposition (5 mm/min) at ca. 80% of the collapse pressure. These parameters were determined prior to the LB-film deposition in a separate experimental run.

After drying at 50°C in air, the samples covered with LB-film were exposed to pulses of a Kr-F UV excimer laser (λ=248 nm).

The laser spot was mapped before the treatments in order to reveal the intensity distribution. It was carried out with a GaP UV-photodiode indirectly by using a quartz plate that reflects ~4% of the incoming intensity. The intensity distribution was measured by scanning the board in 1 mm steps and recording the response voltage by an oscilloscope that was synchronized to the laser.

A single pulse with a pulse length of 30 ns was applied for the treatment of each sample, so that the silica nanospheres don't change during the treatment.

After the laser treatment the LB films were removed by acetone in an ultrasonic bath. The structure and morphology of the samples were characterized by Atomic Force Microscopy (AFM) and Transmission Electron Microscopy (TEM). Samples for TEM were prepared by mechanical and ion beam thinning.

The phenomena occurring at our experimental conditions were computer simulated with the help of Crystalwave [10]. The refractive index (n) and absorption coefficient ($\alpha=4\pi k/\lambda$, where k is the extinction coefficient) of our AlO_x layers were determined by a Woollam M2000DI rotating compensator spectroscopic ellipsometer.

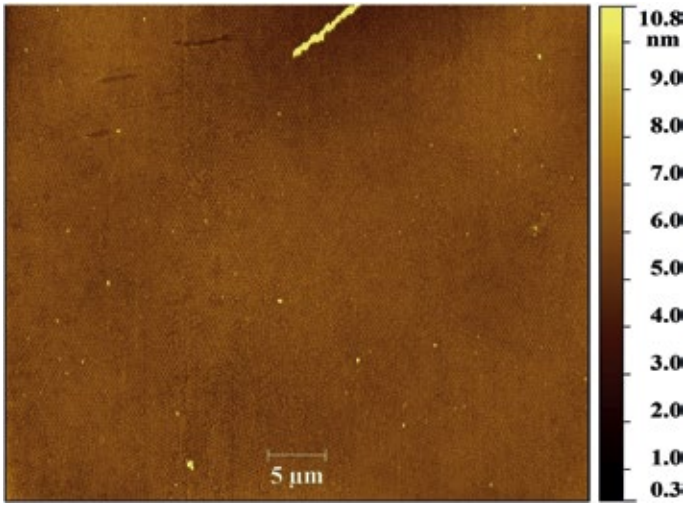

Fig. 1: AFM image of the formed uniform pattern of holes with domains (~ 70 x 70 µm² area).

Janos Szivos

Results

The intensity distribution of the laser spot is roughly Gaussian-like as it is plotted in the color map in figure 2a. In order to obtain reasonably uniform patterns in the AlO_x samples, the inner part (5 x 9 mm²) of the spot, marked with a rectangle in figure 2a, was chosen for the treatment, while the outer regions were masked out.

The intensity of the actual area of the laser spot was estimated to be uniform in our computer simulations. The two parameters at 248 nm wavelength (n=1.681 ± 0.005 and α = (3.86 ± 0.15) x

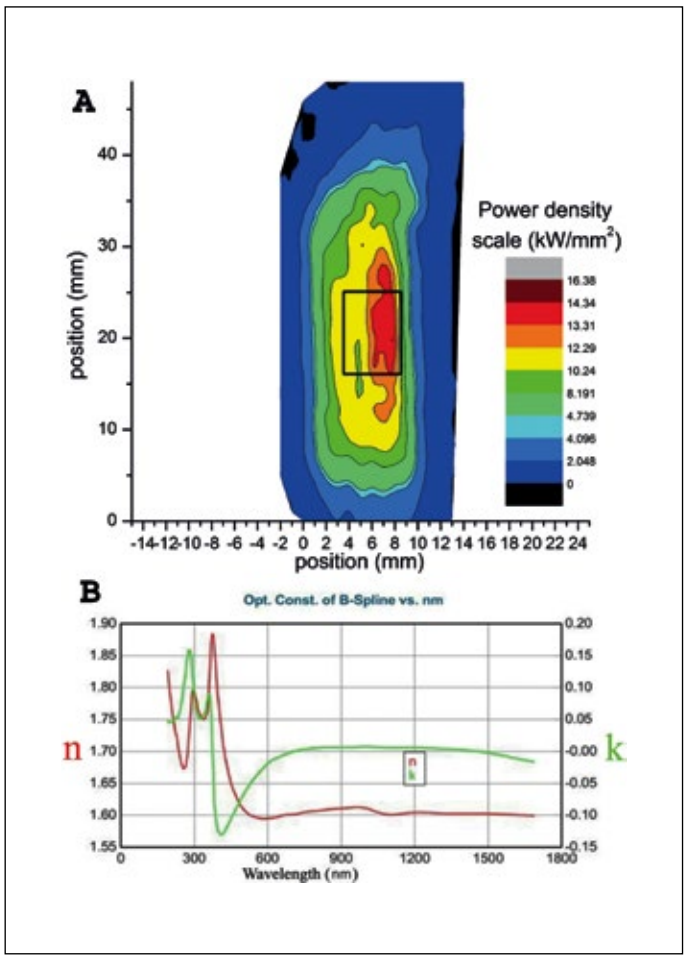

Fig. 2: (a) The color map of the obtained intensity distribution of the laser spot. The black rectangle marks the part of the spot that passes through the aperture. (b) Refractive index and absorption coefficient of our AlO_x layers relative to the wavelength. The n and α values used in our simulations were taken from this data at λ = 248 nm.

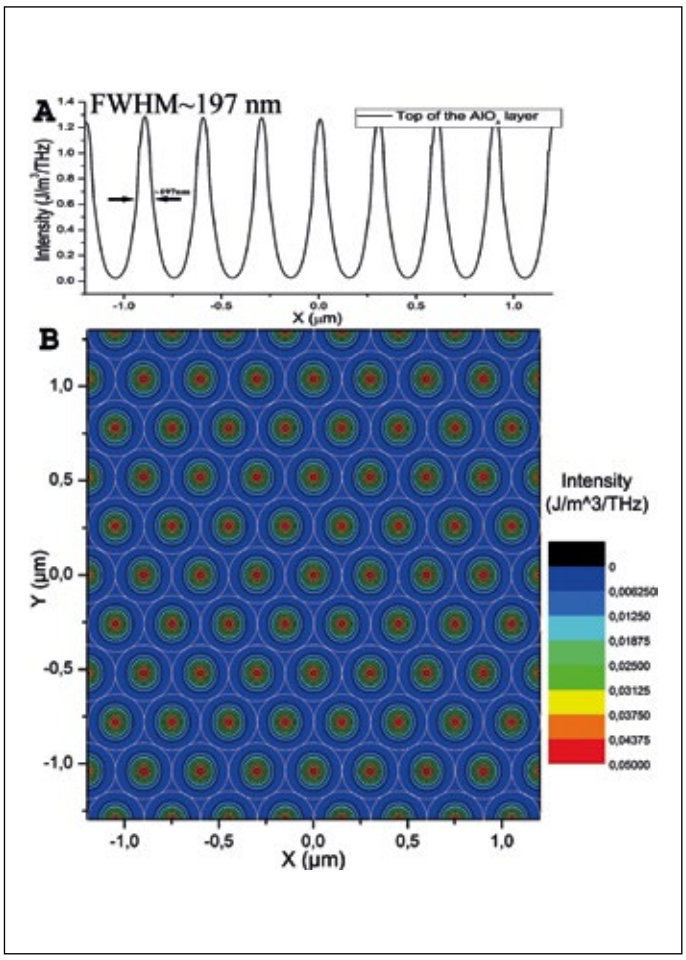

Fig. 3: (a) Simulated intensity profile at the top of the AlO_x layer. (b) The focusing effect of the silica LB film: simulated lateral intensity map. The intensity scales up from blue to green color.

10^4 cm^{-1} as shown in figure 2b were taken from the data obtained by ellipsometry.

The simulations have shown that the silica nanospheres of the LB film can act as individual lenses that focus the incoming laser light (fig. 3). According to the calculations the energy density of the laser light increases with an order of magnitude at the focus of the silica nanolenses (fig. 3 b). This way, extreme local heating may occur beneath every single silica nanosphere that enables the modification of the sample and the preparation of ordered nanoscale patterns.

The total energy of the laser pulse has been varied; the corresponding fluences were calculated considering the Gaussian shape of the whole spot.

Uniform, hexagonally structured pattern of pits were found by AFM, according to the depth profiles, the lateral size of the pits is 220 ± 30 nm in every case.

The sample treated with 30 ± 0.7 mJ/cm^2 (fig. 4) shows the deepest (1.3 ± 0.2 nm) pits and the wall of the holes and the surface is flat and uniform relative to the other samples.

An XTEM image of the sample treated with 35 ± 0.7 mJ/cm^2 fluence near to optimum is shown in figure 5. The cross-section of a single pit is seen here showing ~210 nm diameter and ~3 nm depth. A 15-20 nm wide crystallized region is recognized at the deepest part of the pit.

Discussion

We observed regular patterns of nano-pits formed in AlO_x due to the focusing effect of self-assembled silica nanospheres on the laser spot. The nanospheres act as individual spherical lenses that focus the laser light beneath them as shown by simulations (fig. 3).

Full width at half maximum of the simulated intensity distribution beneath a nanosphere is around 200 nm (fig. 3a). The size (~ 220nm) of the pits observed by AFM is in good agreement with this, confirming the focusing effect. The AFM results helped us to find the optimum fluence that was 32 ± 2 mJ/cm^2. In this case the pits are 1.3 nm deep, and their wall is flat (fig. 4). With the optimum fluence, uniform patterns of pits were prepared in domains that extend at least to 250 x 250 μm^2 areas as it is seen in figure 1. Our LB film consists of domains of ~ 50 μm^2 size, which are replicated to the created patterns.

Wide and shallow pit geometry can be observed by cross-sectional TEM. The typical pit, shown in figure 5, exhibits ~ 210 nm width and ~ 3 nm depth. Beneath the deepest part of some of these pits one can see contrast changes of 20 nm size, which are thought to be the sign of crystallization due to the focused intensity. The AlO_x layer was patterned with few nm deep pits. According to the relatively low absorption coefficient (α), the intensity drop of the laser radiation is only 9.2 ± 0.7 % in the layer. So the deposited energy couldn't be high enough to evaporate the AlO_x. We suggest that our amorphous AlO_x films contain necessarily nanovoids stabilized by electrically ac-

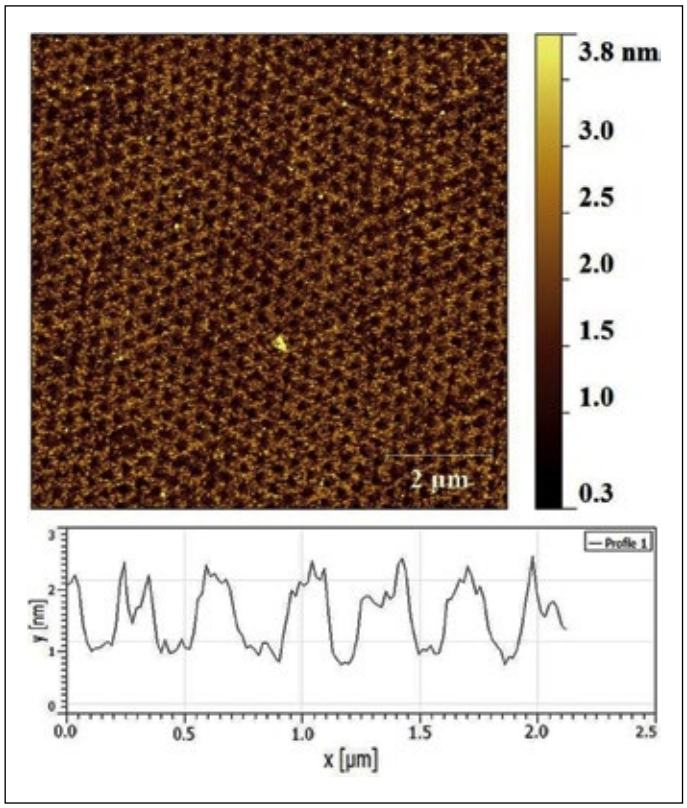

Fig. 4: AFM image and the profile of the pattern of pits obtained (~ 6 x 6 µm² area) by a treatment with fluence of 30 ± 0.7 mJ/cm².

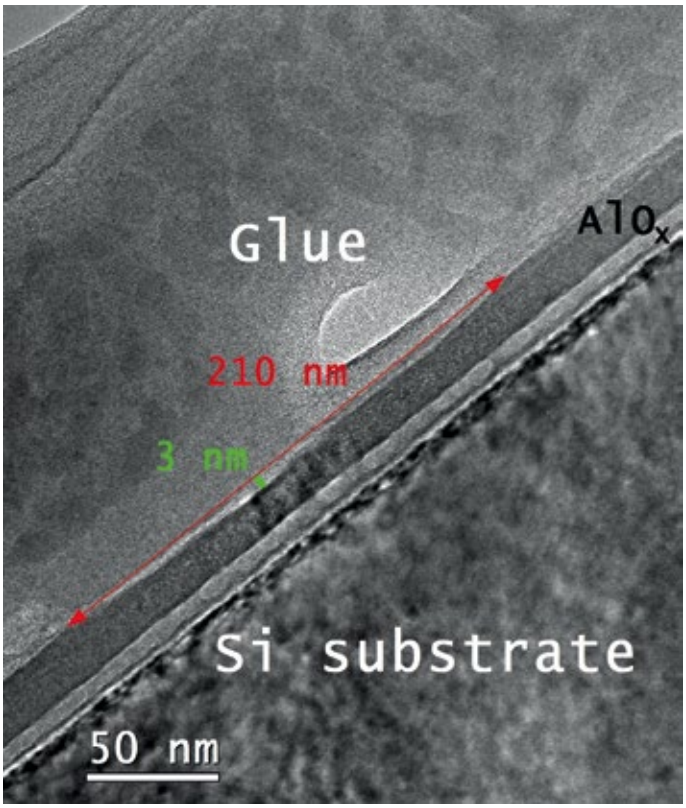

Fig. 5: Cross-sectional TEM image of the sample treated with 35±0.7 mJ/cm² fluence. The cross-section of a pit can be seen in the figure.

tive dangling bonds at their inner surfaces. It is supposed that the voids collapse by the shock wave of the electromagnetic field of the laser pulse. This results in a local densification of the AlO_x and the formation of the shallow pits.

Conclusions

Nanoscale patterning of amorphous AlO_x films was successfully carried out by laser-treating the samples through self-assembled silica nanospheres. Large area of at least 250 x 250 µm² was patterned uniformly in domains (fig. 1). The focussing effect of the nanospheres was confirmed with simulations, which is in good agreement with the observed width of the formed nanopits.

Our results suggest that by applying UV laser technique at carefully controlled conditions molds can be fabricated suitable for nanoimprinting. Alternatively, the patterned surface could act as a mask after a well-chosen etching. The method allows direct nanopatterning of various thin films as well. Further decrease of the sphere size of the LB film below the wavelength of the laser, is supposed to enable the preparation of ordered patterns with periods less than 100 nm via the near field enhancement effect.

Acknowledgements

Z. Szabó and B. Fodor are acknowledged for the help with the simulations and ellipsometry. This work was partially supported by the National Development Agency grant TÁMOP-4.2.2/B-10/1-2010-0025.

References

[1] Kim H. N. *et al.*: Adv. Drug Deliv. Rev., 65, 4, 536–558 (2013)
[2] Bhushan B.: Microelectronic Engineering, 84, 3, 387–412 (2007)
[3] Boltasseva A. *et al.*: Metamaterials 2, 2, 1, 1–17 (2008)
[4] Noh J.-S. *et al.*: Current Appl. Phys., 11, 4, Suppl., S33–S35 (2011)
[5] Guo L. J.: Adv. Materials, 19, 4, 495–513 (2007)
[6] Haynes C. L. *et al.*: J. Phys. Chem. B, 105, 5599–5611 (2001)
[7] Whitesides G. M. *et al.*: Science, 254, 5036, 1312–1319 (1991)
[8] Schwartz D. K.: Surface Science Reports, 27, 7–8, 245–334 (1997)
[9] Deák A. *et al.*: Colloids and Surfaces A: Physicochemical and Engineering Aspects, 278, 1-3, 10-16 (2006)
[10] www.photond.com/products/crystalwave.htm

Contact
János Szívós
Eszter Gergely-Fülöp
Dr. Miklós Serényi
Dr. György Sáfrán
Hungarian Academy of Sciences
Research Centre for Natural Sciences
Institute for Technical Physics and Materials Science
Budapest, Hungary
szivos.janos@ttk.mta.hu
www.mfa.kfki.hu/en